



The sensitivity of the SPEI to potential evapotranspiration and precipitation at multiple timescales on the Huang-Huai-Hai Plain, China

Weijiao Wang^{1,2} · Bin Guo^{1,2} · Yuqing Zhang³ · Liguozhang⁴ · Min Ji^{1,2} · Ying Xu^{1,2} · Xuliang Zhang⁵ · Yanwei Zhang⁶

Received: 12 May 2020 / Accepted: 15 September 2020 / Published online: 6 October 2020
© Springer-Verlag GmbH Austria, part of Springer Nature 2020

Abstract

The standardized precipitation evapotranspiration index (SPEI) is considered appropriate for drought assessment. In this study, changes in drought characteristics and the sensitivity of SPEI to variations in potential evapotranspiration (PET) and precipitation (P) were detected at different timescales (1, 3, 6, and 12 months) on the Huang-Huai-Hai Plain in China from 1901–2015. The results showed that obvious wetting trends were found in this plain and higher SPEI values that were mostly located in the north. Additionally, the SPEI values showed a wetting trend across 83.4%, 99.6%, 98.6%, and 86.6% of the plain at the 1-month (SPEI-01), 3-month (SPEI-03), 6-month (SPEI-06), and 12-month (SPEI-12) timescales, respectively. Obviously, the SPEI displayed a stronger correlation with P than the PET, which was primarily due to the complicated SPEI calculation process. These findings provide critical guidance for sustainable ecological development with the use of the SPEI to detect the impacts of climate factors on drought.

1 Introduction

The global mean surface temperature has increased by 0.85 °C from 1880 to 2012 (IPCC 2013). Under the background of global warming, the occurrence of extreme events has increased (Chen et al. 2017; Guo et al. 2016; Peña-Gallardo et al. 2018). As one of the most damaging and widespread extreme events, drought negatively affects water resources, ecosystems, agricultural production, and sustainable socio-economic development (Deng and Chen 2016; Fu et al.

2019; Wang et al. 2019). Drought is a complicated phenomenon influenced by the integrated effects of multiple factors (Guo et al. 2018).

The droughts have raised enormous concern regarding the occurrence, magnitude, and impacts of drought (Zhang et al. 2017). Numerous specialized drought indices have been proposed and applied for drought monitoring and assessment, e.g., the Palmer drought severity index (PDSI) (Palmer 1965), the standard precipitation index (SPI) (McKee et al. 1993), and the standardized precipitation evapotranspiration index (SPEI) (Vicente-Serrano et al. 2010a). Considering the necessity of assessing drought at multiple timescales, the SPI was developed for drought monitoring and analysis (Vu et al. 2015). Nevertheless, the calculation of SPI is based only on precipitation data and does not consider atmospheric evaporative demand (Zhu et al. 2015). SPEI combines the sensitivity of the PDSI to changes in evaporative demand with the multitemporal nature of the SPI (Vicente-Serrano et al. 2018). Recently, the SPEI has been widely used to study the variability and impacts of drought under warming conditions in many regions of the world (Ayantobo et al. 2017; Deo and Sahin 2015; Manzano et al. 2019). SPEI is an effective tool for monitoring systems that provide important information to improve disaster management (Li et al. 2019; Zhang et al. 2019b).

Drought is influenced by multiple factors, such as potential evapotranspiration (PET), precipitation (P), temperature, and

✉ Bin Guo
guobin07@mails.ucas.ac.cn

¹ Key Laboratory of Geomatics and Digital Technology of Shandong Province, Shandong University of Science and Technology, Qingdao 266590, China

² College of Geomatics, Shandong University of Science and Technology, Qingdao 266590, China

³ School of Urban and Environmental Science, Huaiyin Normal University, Huai'an 223300, China

⁴ Shandong Provincial Institute of Land Surveying and Mapping, Jinan 250102, China

⁵ School of Tourism and Geography Science, Qingdao University, Qingdao 266071, China

⁶ Business School, University of Jinan, Jinan 250002, China

total water storage (Ding et al. 2011). PET and P are key hydroclimatic variables that can directly affect floods, droughts, and water resources (Zhang et al. 2019b). The spatiotemporal variations in PET and P are essential to changes in a climate system (Yang et al. 2019; Yuan et al. 2019). The SPEI is based on PET and P, detecting drought conditions (Beguería et al. 2014; Vicente-Serrano et al. 2010a). Vicente-Serrano et al. (2010a) showed that the SPEI was more sensitive to P than to PET globally. The SPEI relies on two assumptions: the variability of PET and that of P (Vicente-Serrano et al. 2010b). At present, an increasing number of studies are using the SPEI to evaluate drought severity at different timescales (Gouveia et al. 2016; Liu et al. 2017). For example, Yao et al. (2018) applied 3-month, 6-month, and 12-month timescales of SPEI to describe meteorological, agricultural, and hydrological droughts in Xinjiang, China. Liu et al. (2017) studied the response of vegetation to meteorological drought at different timescales. Thus, to better investigate the correlation of SPEI with PET and P, it is meaningful to conduct a comprehensive analysis at multiple timescales.

The Huang-Huai-Hai Plain is one of the major grain production regions in China (Li et al. 2017) and is very prone to drought. Wang et al. (2015) found that the annual drought severity and duration both presented decreasing trends on the Huang-Huai-Hai Plain. Li et al. (2017) pointed out that the plain had experienced reduced droughts of shorter duration and of weaker severity and intensity. However, drought is expected to increase in frequency, duration, severity, and intensity from 2010–2099 under the future representative concentration pathway 8.5 (high emission) scenario. Dai et al. (2020) also suggested that most irrigation districts would experience extended drought durations over the Huang-Huai-Hai Plain under the RCP 8.5 scenario. Therefore, understanding drought characteristics and the sensitivity of drought to climate change is essential for reducing agricultural vulnerability in this region (Mei et al. 2013; Yang et al. 2015).

The primary objective of this study is to explore the spatiotemporal variations of droughts based on the SPEI from 1961–2015. The correlations of SPEI to PET and P were also analyzed at different timescales. A good understanding of the behavior of drought on the plain will be achieved by this study, and useful information for environmental protection and socioeconomic development will be provided.

2 Materials and methods

2.1 Study area

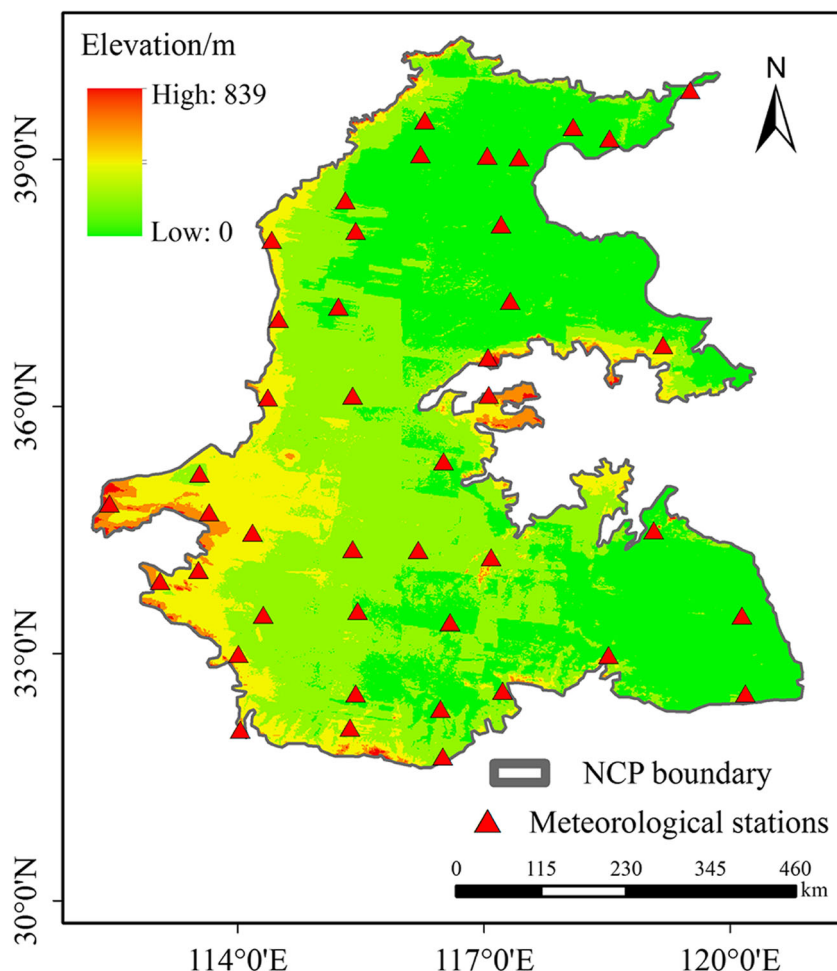
The Huang-Huai-Hai Plain, with an area of 3×10^5 km², is the second-largest plain in China. It is located in the eastern part of China, ranging from 31° 36' N to 40° 29' N and 112° 13' E to 120° 53' E (Fig. 1) (Xu et al. 2019). The plain covers many

highly populated areas in five provinces (Hebei, Shandong, Henan, Anhui, and Jiangsu) and two administrative cities (Beijing and Tianjin) (Wu et al. 2019). It is mainly formed by the sedimentation and river source effects of the Yellow River, Huaihe River, Haihe River, and Luanhe River (Liu et al. 2018). The downstream region of the Yellow River extends across the central plain and divides it into two parts: the Haihe Plain in the north and the Huanghuai Plain in the south (Hu et al. 2010). The area is located in a warm temperate zone with a strong impact from the East Asian Monsoon (Xiao et al. 2018). The annual mean precipitation is approximately 500–900 mm. Due to the continental monsoon climate, precipitation mainly occurs in summer, with less precipitation in spring and winter. The annual mean temperature on the plain ranges between 8 and 15 °C (Chen et al. 2019b). Additionally, two of the major provinces, Henan and Shandong, have been facing a dramatic decreasing trend in total water resources starting in the twenty-first century (Wang et al. 2019; Zhou et al. 2020). The amount of total water resources in Hebei Province has changed little, but the approximately 1.8×10^{10} m³ of reserve water is still far less than the average on the plain (Su et al. 2020; Yang et al. 2016). This indicated that Hebei Province has frequently been subjected to droughts (Shiau et al. 2007). The plain has a flat terrain with loam and sandy soil types, as the alluvial plain has mainly developed through the intermittent flooding of the Yellow River (Ye et al. 2012). It is the main production area for agricultural crops in China, which makes the plain an ideal test location for monitoring droughts and their ecological and economic impacts (Xiao et al. 2014).

2.2 Data

The SPEI used in this study was derived from SPEIbase v2.5 (<http://spei.csic.es/database.html>). SPEIbase v2.5 is based on CRU TS 3.24.01 input data from the Climatic Research Unit (CRU) of the University of East Anglia (http://badc.nerc.ac.uk/browse/badc/cru/data/cru_ts_3.24.01). This dataset has the timescales between 1 and 12 months with a spatial resolution of $0.5^\circ \times 0.5^\circ$, and its temporal coverage is between January 1901 and December 2015. The calculation of the PET in SPEIbase v2.5 is based on the FAO-56 Penman-Monteith method. P data were obtained from the CRU TS3.24.01 dataset. Um et al. (2020) showed that PET was predominant in drought phenomena in various geographic regions based on data from CRU and the National Centers for Environmental Prediction (NCEP). The results obtained from the two datasets appear to be slightly different. Van der Schrier et al. (2013) calculated the self-calibrating PDSI for the period 1901–2009 based on the CRU TS 3.10.01 datasets and found a trend toward drying conditions in some parts of the world during 1950–1985.

Fig. 1 DEM and meteorological stations on the Huang-Huai-Hai Plain



We used observed data to verify the reliability of SPEIbase v2.5 data in terms of spatiotemporal performances of SPEI in the plain. The SPEI was calculated based on the monthly precipitation and temperature from 43 meteorological stations during 1961–2015. The monthly precipitation and temperature were obtained from the China Meteorological Data Service Center (<http://data.cma.cn>).

2.3 Methods

2.3.1 Mann–Kendall nonparametric test

The Mann–Kendall (M–K) test is based on the correlation between the relative ranking of values in a time series and their chronological order (Kendall 1975; Mann 1945). The M–K test is widely used to detect trends in hydrometeorological time series, such as trends in P, PET, temperature, and drought index (Ye et al. 2019; Zhao et al. 2019). The M–K statistic S is used to estimate the significance as follows (Dietz 1981; Hirsch et al. 1982; Lettenmaier 1988):

$$S = \sum_{i=1}^{n-1} \sum_{j=i+1}^n \text{sgn}(x_j - x_i) \tag{1}$$

$$\text{sgn}(\theta) = \begin{cases} 1 & (\theta > 0) \\ 0 & (\theta = 0) \\ -1 & (\theta < 0) \end{cases} \tag{2}$$

where x_j and x_i are continuous information values; n is the size of the dataset. The variance of the statistic S is as follows:

$$\text{var}(S) = \frac{n(n-1)(2n+5) - \sum_{p=1}^q t_p(t_p-1)(2t_p+5)}{18} \tag{3}$$

where q is the number of tied groups and t_p is the size of the p th item in the m group. S is expected to have an $N(0, \text{var}(S))$ distribution (Jung et al. 2011).

The Mann–Kendall test statistic Z_{MK} is estimated as follows:

$$Z_{MK} = \begin{cases} \frac{s-1}{\sqrt{\text{var}(S)}}, & S > 0 \\ 0, & S = 0 \\ \frac{s+1}{\sqrt{\text{var}(S)}}, & S < 0 \end{cases} \quad (4)$$

where Z_{MK} is a standard normal variable. An above zero (below zero) value of Z_{MK} illustrates that the data show a positive (negative) trend over time. The null hypothesis H_0 , that Z_{MK} is not statistically significant or shows no significant trend, accepted if $-Z_{1-\alpha/2} \leq Z_c \leq Z_{1-\alpha/2}$, where $\pm Z_{1-\alpha/2}$ are the standard normal deviates and α is the significance level for the test (Jung et al. 2011; Zhao et al. 2019).

2.3.2 Pearson's correlation analysis

To evaluate the correlation of climate factors to variations in SPEI, the spatial correlations between the SPEI and the driving factors of drought were examined by calculating Pearson's correlation coefficient for all grid cells (Xu et al. 2006).

3 Results

3.1 Comparison between SPEIbase v2.5 and the observed SPEI

The Pearson correlation coefficient (R), mean absolute error (MAE), and normalized root mean squared error (NRMSE) were used to quantitatively compare the performance of the SPEIbase v2.5 and observed SPEI at different timescales (Fig. 2). R was used to evaluate the degree of correlation between the SPEIbase v2.5 and the observed SPEI. The MAE reflects the average error between the SPEI product and the observed SPEI. NRMSE refers to the normalized root mean square deviation or error. When the value is close to zero, it represents less errors. When the NRMSE was higher than 0.3, the product estimates were considered unreliable. The results showed that the four groups of data presented significant linear correlations (Fig. 2), with correlation coefficients of 0.89, 0.88, 0.88, and 0.87, respectively. SPEI-01 had the highest correlation coefficient (0.89), compared with those of the other three timescales (Fig. 2a). In addition, SPEI-01 had the lowest NRMSE (0.07) and the smallest MAE (0.34) among the four timescales. Compared with those of SPEI-01, SPEI-03 and SPEI-06 had higher MAE and NRMSE, and slightly lower R (0.88). SPEI-12 exhibited a higher NRMSE (0.12) and the highest MAE (0.39), indicating that gridded SPEI-01 performed better than SPEI-12 (Fig. 2a, d). Overall, the SPEIbase v2.5 values were significantly correlated with the observed SPEI and demonstrated good spatial performance.

Figure 3 shows the temporal performances of SPEIbase v2.5 compared with the observed SPEI at the four timescales

during 1961–2015. SPEIbase v2.5 correctly reflected the general patterns of the four timescale variations in the observed SPEI during 1961–2015. In particular, SPEI-01 and SPEI-03 from SPEIbase closely followed the fluctuations of the observed SPEI and exhibited strong temporal similarity (Fig. 3a, b). Thus, SPEIbase v2.5 can be applied to analyze spatio-temporal variations in drought intensity and the sensitivity of the SPEI to climate factors in the study area.

3.2 Temporal-spatial variations in droughts

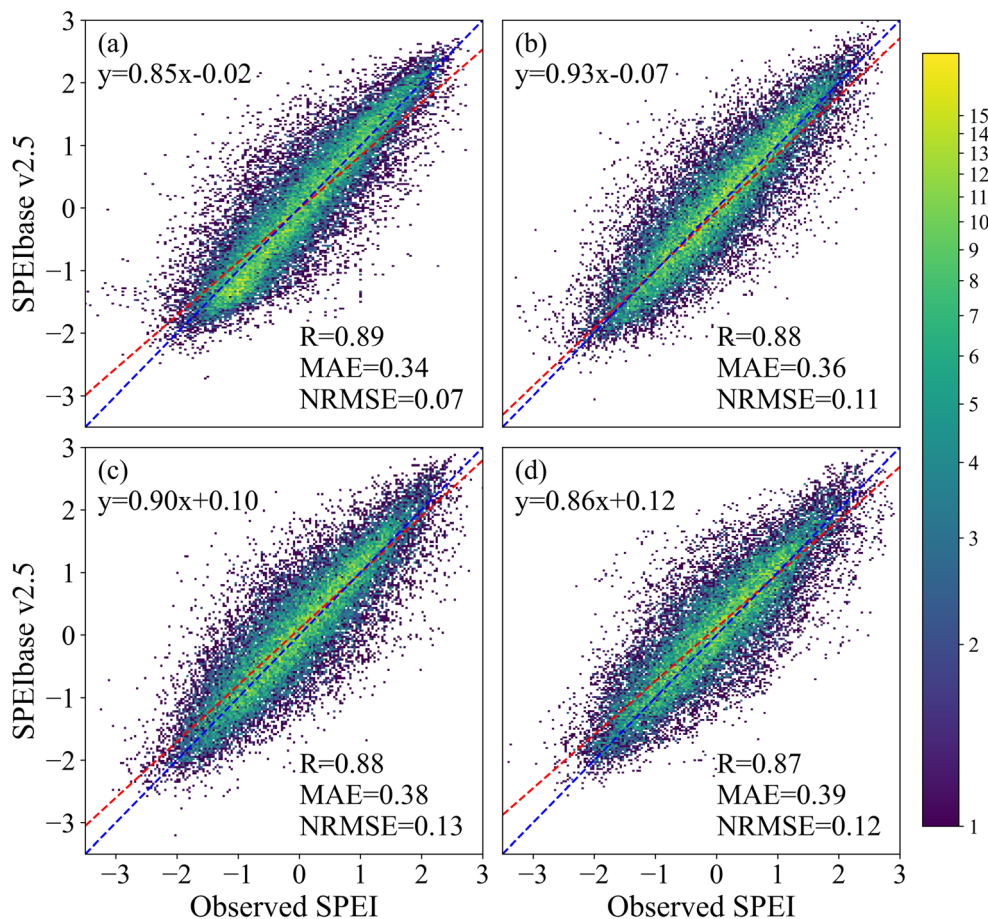
Figure 4 shows the temporal evolution of the SPEI based on grids at different timescales from 1901 to 2015 (i.e., SPEI-01, SPEI-03, SPEI-06, and SPEI-12). The fluctuations in SPEI-01 were frequent, without considering the influence of relatively longer preceding precipitation, and were susceptible to rapid climatic variations (Fig. 4a). The amplitudes of the SPEI-03, SPEI-06, and SPEI-12 fluctuations in the time series were smaller than those of the SPEI-01 fluctuations in the time series (Fig. 4b, c, d). As the timescale increased, the amplitude and the frequency of the fluctuations decreased, indicating that the separations between dryness and wetness became clearer (Fig. 4). Changes of precipitation and temperature can make the SPEI fluctuate, which is a reasonable sign of drought conditions (Du et al. 2013; Wang et al. 2018).

According to the classification of SPEI values, an SPEI value between -2 and -1.5 is defined as severe drought, and a value below -2 is defined as extreme drought at a given station/grid. At the 1-month and 3-month timescales, numerous SPEI values were between -2 and -1.5 . Among them, the SPEI values reached their lowest values in 2001 (SPEI-01) and 1917 (SPEI-03), at -1.76 and -1.92 , respectively (Fig. 4a, b). At the 6-month timescale, the lowest value was -2.27 in 1916, representing extreme drought conditions (Fig. 4c). Severe drought also occurred in 1919 at the 12-month timescale, reaching -1.96 (Fig. 4d). These results clearly indicate severe drought conditions occurred around the 1920s according to 3-, 6-, and 12-month SPEI.

Figure 5 shows the spatial pattern of the SPEI at various timescales from 1901 to 2015, displaying distinct distribution characteristics from north to south. As the timescale increased, the value of SPEI decreased from 0.006–0.014 (SPEI-01) to -0.004 – -0.007 (SPEI-12) (Fig. 5a, d). The SPEI values were low in the middle and southern part of the plain at each timescale. In contrast, high SPEI values were located in the north (Fig. 5a–d).

The Mann–Kendall method and Sen's slope were applied to detect trend variations in each grid from 1901 to 2015 on the plain (Fig. 6). The spatial variations of SPEI-01, SPEI-03, SPEI-06, and SPEI-12 showed local drying trends (16.6%, 0.4%, 1.4%, and 13.4% of the plain, respectively) and wetting trends (83.4%, 99.6%, 98.6%, and 86.6% of the plain, respectively) during 1901–2015. The spatial pattern of SPEI-01 was

Fig. 2 Evaluation of the performance of SPEIbase v2.5 on the Huang-Huai-Hai Plain during 1961–2015. **a** 1-month, **b** 3-month, **c** 6-month, and **d** 12-month timescales. The blue and red oblique dash lines denote a 1:1 line and a least-squares regression line, respectively



relatively complex. A drying trend was obvious in the western region (Fig. 6a). Specifically, the southern part of this region presented a significant wetting trend with relatively large slope values at the SPEI-03 and SPEI-06 timescales (Fig.

6b, c). The slope values of the 12-month SPEI obviously decreased in the northern part of the plain but the slope values in the southern region increased (Fig. 6d). It can be concluded that more than 70% of the total grids experienced wetting

Fig. 3 The temporal comparison of the monthly SPEI from SPEIbase v2.5 against the observed SPEI from 1961–2015. **a** 1-month, **b** 3-month, **c** 6-month, and **d** 12-month timescales. The red line represents SPEIbase v2.5, and the blue line represents the observed SPEI

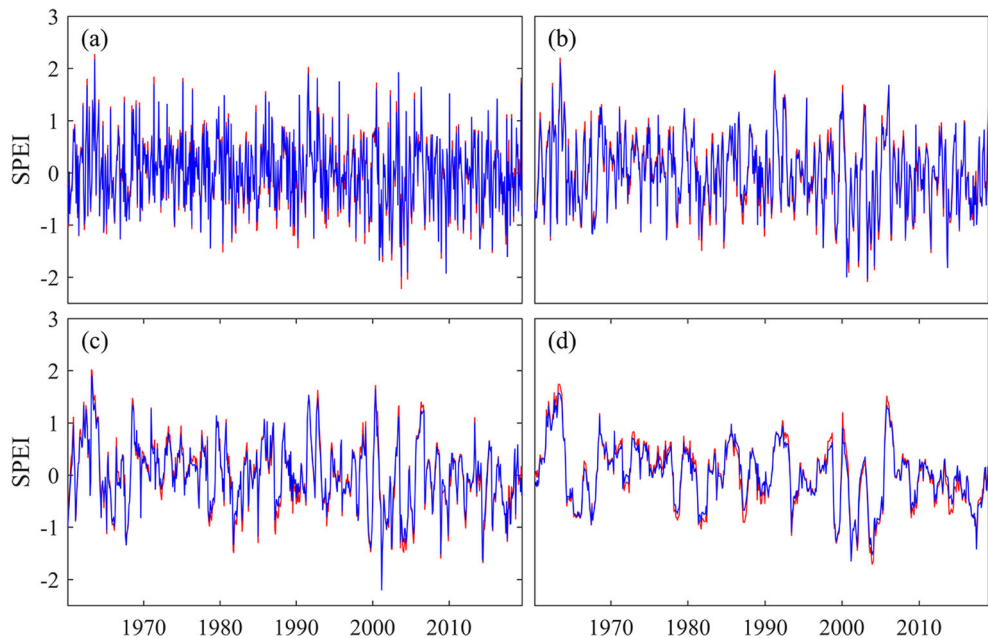


Fig. 4 Temporal variations in SPEIbase v2.5 from 1901–2015 on the Huang-Huai-Hai Plain. **a** 1-month, **b** 3-month, **c** 6-month, and **d** 12-month timescales. The blue line represents the SPEI value, and the red line represents an SPEI value of -1.5

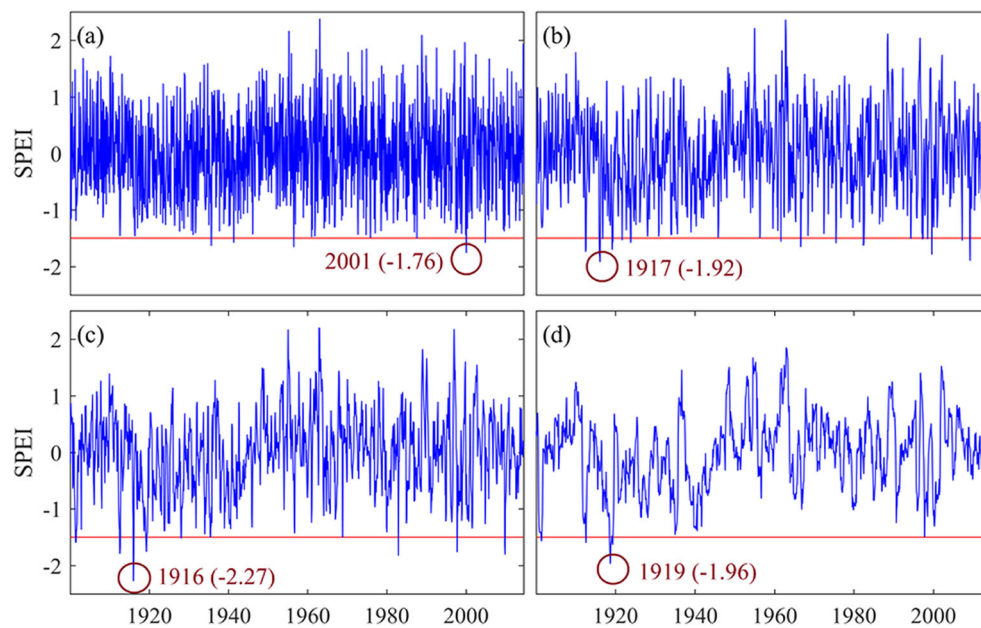


Fig. 5 The spatial pattern of SPEIbase v2.5 from 1901–2015 on the Huang-Huai-Hai Plain. **a** 1-month, **b** 3-month, **c** 6-month, and **d** 12-month timescales

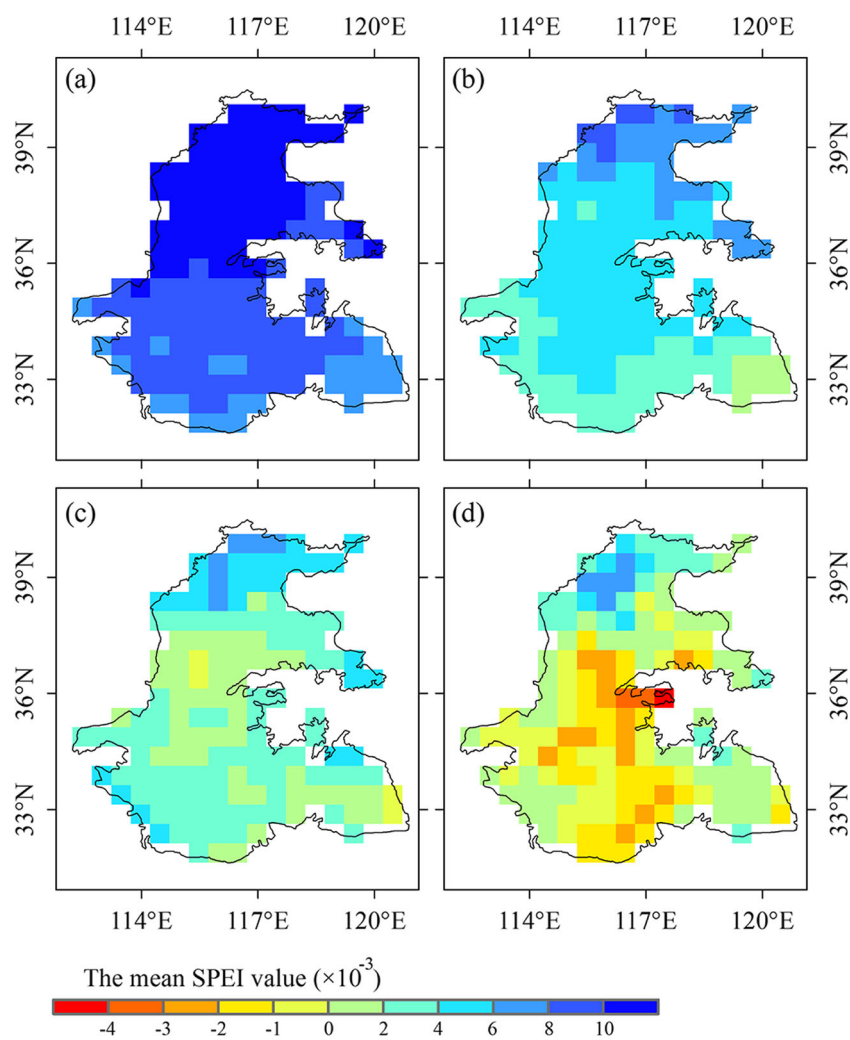
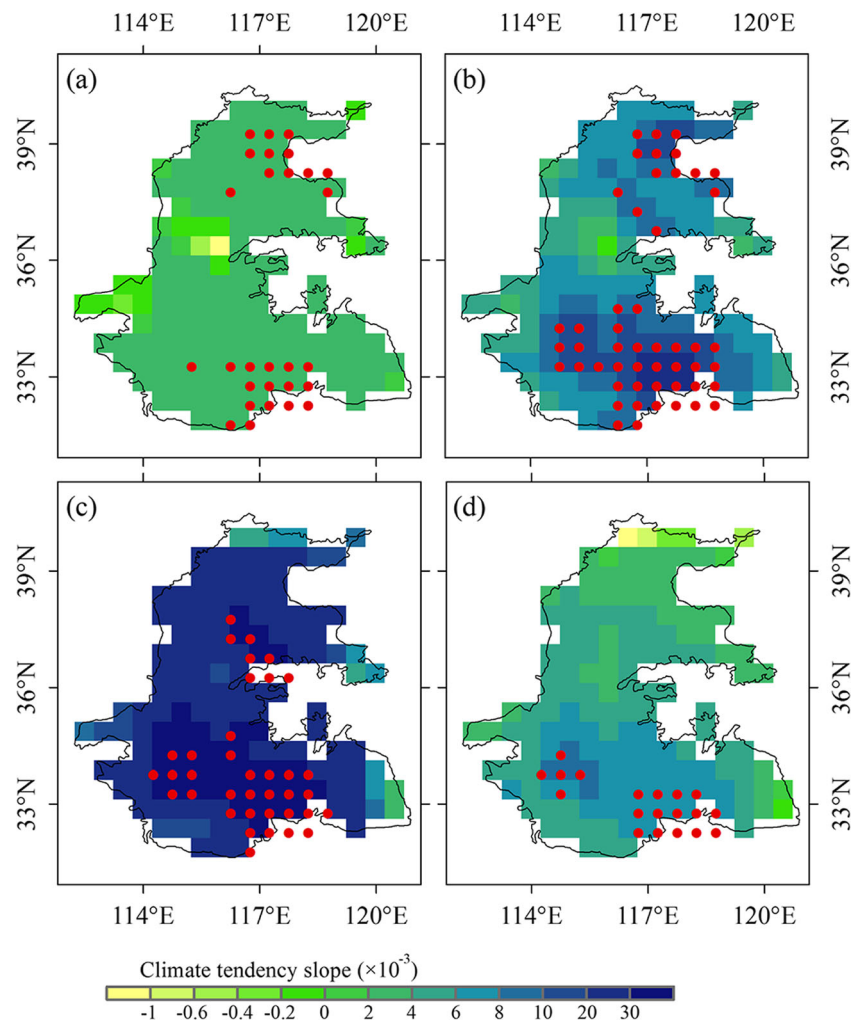


Fig. 6 The spatial pattern of Sen's slope of the SPEIbase v2.5 from 1901–2015 on the Huang-Huai-Hai Plain. The red dot represents that the trend is significant at the 0.05 significance level. **a** 1-month, **b** 3-month, **c** 6-month, and **d** 12-month timescales



trends at each timescale (Fig. 6). The plain with significant wetting trends mainly located in the south, accounting for approximately 9.7% of the total grids for SPEI-01, 23% for SPEI-03, 17% for SPEI-06, and 8.8% for SPEI-12. Twelve-month SPEI characteristics indicated that drying trends existed in the northern parts of the plain. Overall, drought was being alleviated due to the significant wetting trends in most regions. Similar results were found by Wang et al. (2015), who pointed out that the wetting trends may have been caused by increased precipitation under global warming. In addition, the alleviation of drought may be attributed to an increase in aerosols, which decrease solar radiation and reduce PET (Gao et al. 2006).

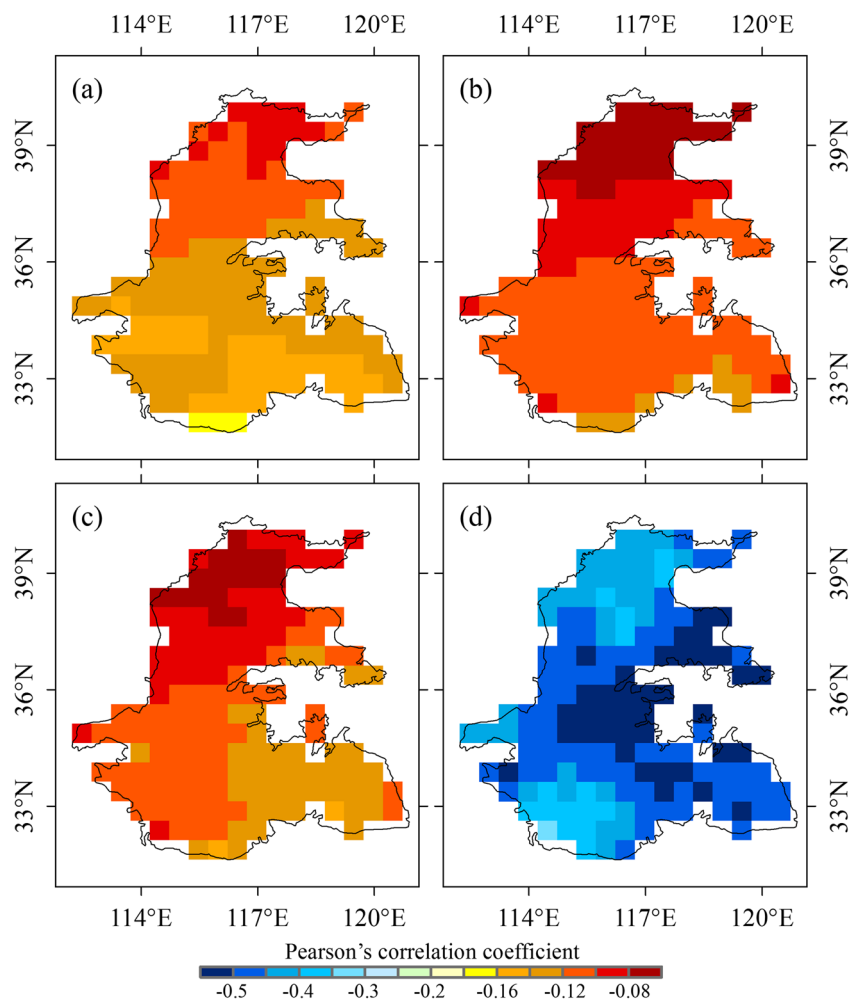
3.3 Influence of PET and P on SPEI

We conducted the sensitivity of the SPEI to PET and P to quantitatively explain the mechanisms of droughts. The sensitivity of the SPEI to PET was assessed as the negative correlation between the SPEI-01, SPEI-03, SPEI-06, and SPEI-

12 with the cumulative 1-month PET, 3-month PET, 6-month PET, and 12-month PET, respectively (Fig. 7). At the 1-, 3-, and 6-month timescales, the SPEI had a low correlation coefficient with PET. At the 12-month timescale, the most significant correlation coefficient was -0.57 at given grids of the eastern plain. All the grids exceeded the 0.05 significance level at the 12-month timescale. The correlation coefficient between SPEI-12 and 12-month PET was the highest, which was determined by the algorithm used to estimate the duration factors for the calculation of the SPEI (Zhang et al. 2019a). Thus, the SPEI was influenced by PET, especially at the 12-month timescale.

Pearson correlation analysis was also conducted between SPEI and P in this study (Fig. 8). At the 1-month timescale, the SPEI and P showed a higher correlation in the southern parts of the plain than in the north, with a correlation coefficient of 0.68. The P in the northern parts of the plain had little impact on SPEI, and the correlation coefficient was 0.35 (Fig. 8a). At the 3-month timescale, the correlation coefficient between the SPEI and P was higher in the south (0.59) than in the north

Fig. 7 Pearson's correlation coefficient between SPEI and PET at different timescales at the grid cell level on the Huang-Huai-Hai Plain during 1901–2015. **a** 1-month, **b** 3-month, **c** 6-month, and **d** 12-month timescales (all grids are at the 0.05 significance level at the 12-month timescale)



(0.30) (Fig. 8b). In terms of the 6-month timescale, the correlation coefficient increased from the north (0.36) to south (0.68) (Fig. 8c). In addition, the highest correlation coefficient of approximately 0.99 expanded to cover almost all regions of the study area at the 12-month timescale (Fig. 8d). As the timescale changed from 1 to 12 months, the correlation coefficient between SPEI and P increased. And the correlation coefficients of 1-, 3-, and 6-month timescales presented similar spatial distribution characteristics, with higher correlation coefficients in the south and lower in the north.

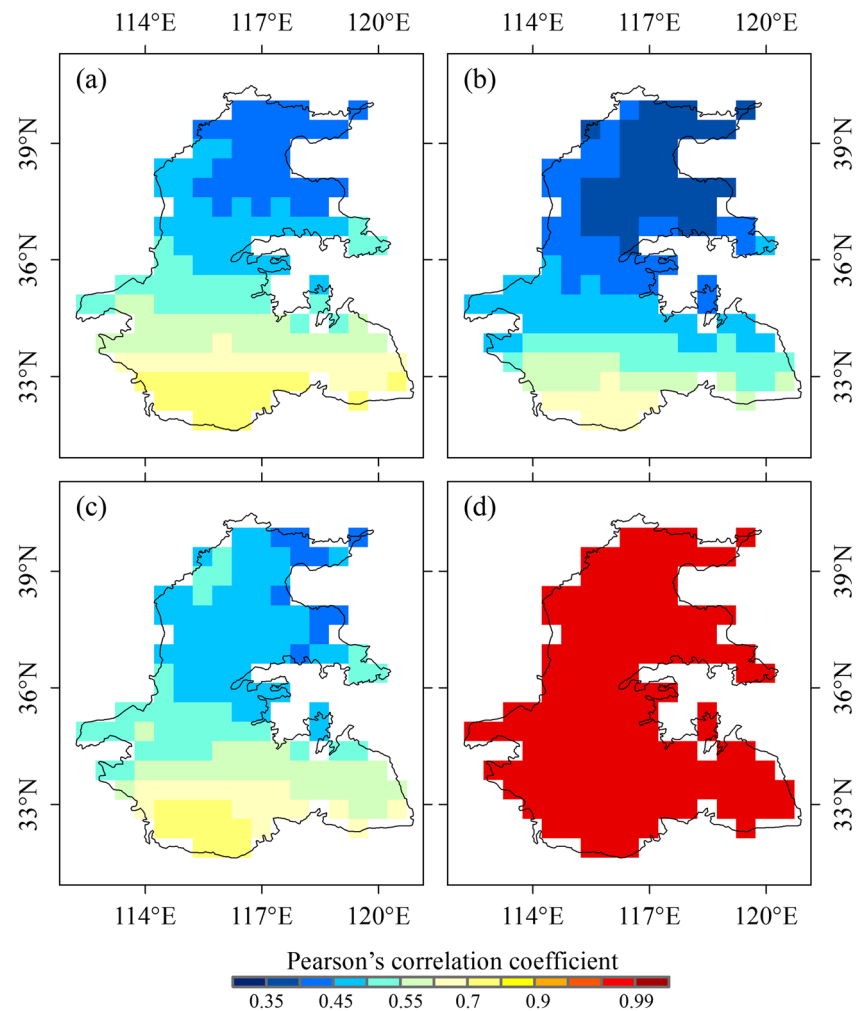
4 Discussion

The SPEI is based on the monthly differences between P and PET, which represents a simple climatic water balance condition (Vicente-Serrano et al. 2010a). The mean Pearson's correlation coefficients between SPEI and PET (or SPEI and P) were compared at different timescales (Fig. 9). Higher correlations were found between the SPEI and P than between the SPEI and PET at the same timescale. The correlation

coefficient between SPEI and PET (and P) on the 12-month timescale was the highest, which indicated that the SPEI was susceptible to PET and P on long timescale. Zhang et al. (2019a) confirmed that the SPEI algorithm can incorporate both PET and P data for an unspecified period but corresponded best to the most recent 9–12 months. Previous conditions were incorporated because the long-term drought was cumulative, so the correlations between SPEI and PET and P at a particular time were dependent on the current and cumulative conditions from previous months (Zhang et al. 2019a). Thus, the SPEI was highly correlated with PET and P at the lengthier timescale.

Figure 10 shows that the spatial characteristics of the SPEI values were related to PET and P at the 12-month timescale. The areas with higher SPEI values were located in the southern parts of the plain (Fig. 10a). Higher P and lower PET values were also observed in the southern parts of the plain (Fig. 10b, c). In certain areas of the southern plain, both the SPEI and P showed significant increasing trends (Fig. 10 d and f). The SPEI, PET, and P all showed upward trends in the southwestern regions (Fig. 10 d, e, and f). The upward trend in

Fig. 8 Pearson’s correlation coefficient between SPEI and P at different timescales at the grid cell level on the Huang-Huai-Hai Plain during 1901–2015. **a** 1-month, **b** 3-month, **c** 6-month, and **d** 12-month timescales (all grids are significant at the 0.05 significance level at the 1-, 3-, 6-, and 12-month timescales)



the SPEI represented a wetting trend. The conditions still tended to represent wetting even with an upward trend in PET. The increasing amount of P might be the cause of the

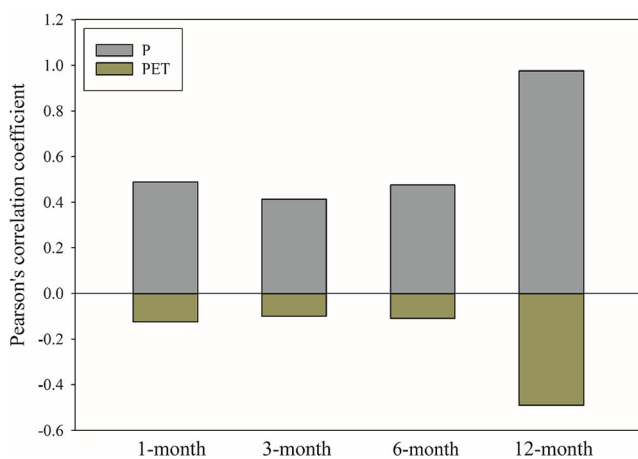


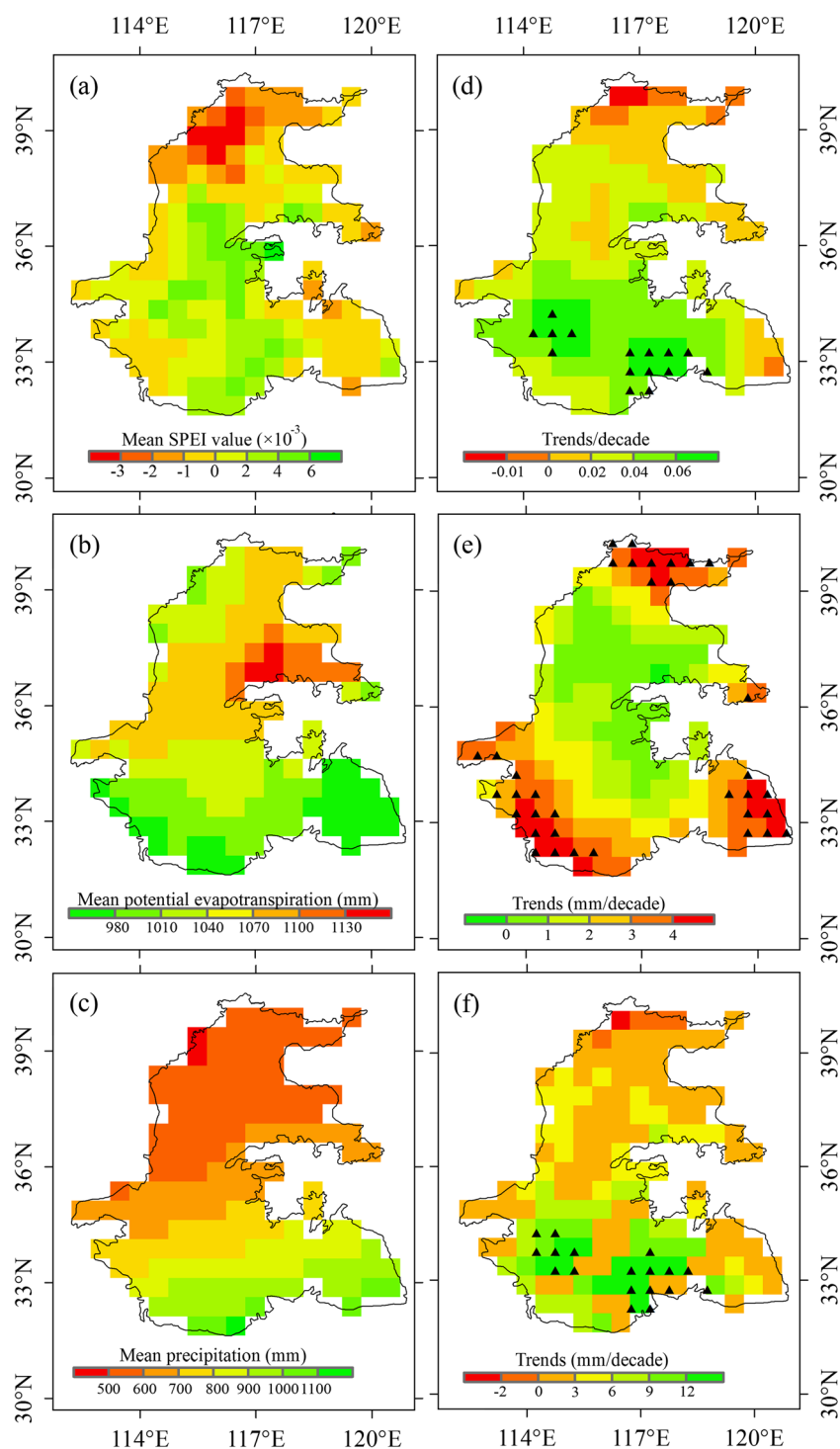
Fig. 9 Mean Pearson’s correlation coefficients between SPEI and P (and PET) at different timescales (1, 3, 6, and 12 months) on the Huang-Huai-Hai Plain

small correlation between SPEI and PET. Yao et al. (2018) confirmed that P was the main factor causing droughts. At the 12-month timescale, the value of SPEI in most areas of the plain might be explained by the diverse hydroclimatic conditions and by the combined effects of PET and P (Vicente-Serrano et al. 2015).

The SPEI was more sensitive to P than to PET on the Huang-Huai-Hai Plain; this was likely because the SPEI included the sensitivity of the changes in the precipitation in its calculation and was influenced by the standardization of anomalies in the soil water budget (Ling et al. 2019). The SPEI may be more sensitive to PET than to P in other areas (Vicente-Serrano et al. 2010a; Zhang et al. 2019b). The correlation of SPEI with either PET or P was not high in certain regions with particular topography, such as areas susceptible to the high altitude, and other variables should also be taken into account (Paulo et al. 2012).

The SPEI can be used to identify drought conditions and to capture the responses of climate variables to drought (Vicente-Serrano et al. 2018). Therefore, multiple climate variables (e.g., runoff, temperature, and soil moisture) may play

Fig. 10 Mean values of **a** SPEI, **b** PET, **c** P, and variation trends in **d** SPEI, **e** PET, and **f** P at the 12-month timescale determined by the Mann–Kendall trend test at the grid cell level on the plain during 1901–2015. The symbol \blacktriangle represents an upwards trend with $p \leq 0.05$



important roles in explaining drought conditions and may have effects on the SPEI (Zhang et al. 2017). There is widespread recognition that global warming increased hydrologic climatic extremes (Chen et al. 2019a; Li et al. 2020). A significant positive correlation was observed between runoff and SPEI (Yao et al. 2018). Minimal runoff, high temperature, and a lack of precipitation led to reductions in soil moisture (Ling et al. 2020; Zhang et al. 2020), which was more likely to

induce drought (Guo et al. 2013). SPEI showed the highest correlation with soil moisture among the different drought indices, e.g., SPI, SPEI, and PDSI (Vicente-Serrano et al. 2012). As the plain was an agricultural region characterized by frequent droughts, both sufficient surface water and groundwater played active roles to ensure food supply (Tang et al. 2018; Wang et al. 2015). The SPEI had a good correlation with surface water and groundwater (Vicente-Serrano

et al. 2012). Notably, other factors should also be considered among the environmental factors related to the SPEI. We mainly focused on the sensitivity of the SPEI to PET and P in this study. A comprehensive consideration of the climate factors associated with the SPEI will improve our understanding of droughts (Marvel et al. 2019). We only used the CRU data in this present study. Various data such as Climate Forecast System Reanalysis (CFSR), Climatologies at High Resolution for the Earth's Land Surface Areas (CHELSA), and European Environment Agency (ERA5) climate reanalysis data produced by ECMWF should also be considered in future studies to compensate for the errors and uncertainties introduced by using only the CRU data.

5 Conclusions

The spatiotemporal characteristics of drought and the sensitivity of SPEI to the related climate factors were investigated based on SPEIbase v2.5 on the Huang-Huai-Hai Plain of China from 1901 to 2015. The SPEI showed high values in the northern parts of the study area, and a significant wetting trend was observed in the southern regions. The changes in P were the dominant driving factors for the SPEI at different timescales. In addition, the correlation coefficients between the SPEI and PET and P were the highest at 12 months on the Huang-Huai-Hai Plain. Overall, the use of the SPEI is beneficial for the assessment and quantification of droughts on the Huang-Huai-Hai Plain in China. The present study provides evidence that improves our understanding of the climate variation related to drought.

Acknowledgments We appreciate the editors and reviewers for their constructive suggestions and insightful comments, which helped us to greatly improve this manuscript. We would like to thank the Climatic Research Unit for providing high-resolution gridded data and the China Meteorological Data Service Center for supplying the meteorological data.

Funding This work was funded by the National Natural Science Foundation of China (41807170), the Major Science and Technology Innovation Projects of Shandong Province (2019JZZY020103), the Talent Introduction Plan for Youth Innovation Team in Universities of Shandong Province (Innovation Team of Satellite Positioning and Navigation), and the Opening Fund of Key Laboratory of Geomatics and Digital Technology of Shandong Province.

References

- Ayantobo OO, Yi L, Song S, Ning Y (2017) Spatial comparability of drought characteristics and related return periods in Mainland China over 1961–2013. *J Hydrol* 550:549–567
- Beguera S, Vicente-Serrano SM, Reig F, Latorre B (2014) Standardized precipitation evapotranspiration index (SPEI) revisited: parameter fitting, evapotranspiration models, tools, datasets and drought monitoring. *Int J Climatol* 34:3001–3023
- Chen ZS, Chen YN, Bai L, Xu J (2017) Multiscale evolution of surface air temperature in the arid region of Northwest China and its linkages to ocean oscillations. *Theor Appl Climatol* 128:945–958
- Chen L, Chen X, Cheng L, Zhou P, Liu Z (2019a) Compound hot droughts over China: identification, risk patterns and variations. *Atmos Res* 227:210–219
- Chen X, Mo X, Zhang Y, Sun Z, Liu Y, Hu S, Liu S (2019b) Drought detection and assessment with solar-induced chlorophyll fluorescence in summer maize growth period over North China Plain. *Ecol Indic* 104:347–356
- Dai C, Qin XS, Lu WT, Zang HK (2020) A multimodel assessment of drought characteristics and risks over the Huang-Huai-Hai River Basin, China, under climate change. *Theor Appl Climatol* 141: 601–613
- Deng HJ, Chen YN (2016) Influences of recent climate change and human activities on water storage variations in Central Asia. *J Hydrol* 544:46–57
- Deo RC, Sahin M (2015) Application of the artificial neural network model for prediction of monthly Standardized Precipitation and Evapotranspiration Index using hydrometeorological parameters and climate indices in eastern Australia. *Atmos Res* 161–162:65–81
- Dietz EJKA (1981) A nonparametric multivariate test for monotone trend with pharmaceutical applications. *J Am Stat Assoc* 76:169–174
- Ding Y, Hayes MJ, Widhalm M (2011) Measuring economic impacts of drought: a review and discussion. *Disaster Prev Manag* 20:434–446
- Du J, Fang J, Xu W, Shi P (2013) Analysis of dry/wet conditions using the standardized precipitation index and its potential usefulness for drought/flood monitoring in Hunan Province, China. *Stoch Env Res Risk A* 27:377–387
- Fu MR, Guo B, Wang WJ, Wang J, Zhao LH, Wang J (2019) Comprehensive assessment of water footprints and water scarcity pressure for main crops in Shandong Province, China. *Sustainability* 11:1856
- Gao G, Chen D, Ren G, Chen Y, Liao Y (2006) Spatial and temporal variations and controlling factors of potential evapotranspiration in China: 1956–2000. *J Geogr Sci* 16:3–12
- Gouveia CM, Trigo RM, Begueria S, Vicente-Serrano SM (2016) Drought impacts on vegetation activity in the Mediterranean region: an assessment using remote sensing data and multi-scale drought indicators. *Glob Planet Chang* 151:15–27
- Guo B, Chen YN, Shen YJ, Li WH, Wu CB (2013) Spatially explicit estimation of domestic water use in arid region of northwestern China. *Hydrol Sci J* 58(1):162–176
- Guo B, Chen ZS, Guo JY, Liu F, Chen CC, Liu KL (2016) Analysis of the nonlinear trends and non-stationary oscillations of regional precipitation in Xinjiang, Northwestern China, using ensemble empirical mode decomposition. *Int J Environ Res Public Health* 13:345
- Guo H, Bao AM, Liu T, Ndayisaba F, Jiang L, Kurban A, De Maeyer P (2018) Spatial and temporal characteristics of droughts in Central Asia during 1966–2015. *Sci Total Environ* 624:1523–1538
- Hirsch RM, Slack JR, Smith RA (1982) Techniques of trend analysis for monthly water quality data. *Water Resour Res* 18(1):107–121
- Hu S, Mo X, Lin Z, Qiu J (2010) Emergy assessment of a wheat-maize rotation system with different water assignments in the North China Plain. *Environ Manag* 46:643–657
- IPCC (2013) Climate change 2013: the physical science basis. Contribution of Working Group I to the Fifth Assessment Report of the Intergovernmental Panel on Climate Change. In: Stocker TF, Qin D, Plattner GK, Tignor M, Allen SK, Boschung J, Nauels A, Xia Y, Bex V, Midgley PM (eds). Cambridge University Press, Cambridge, pp 1535
- Jung IW, Bae DH, Kim G (2011) Recent trends of mean and extreme precipitation in Korea. *Int J Climatol* 31:359–370

- Kendall MG (1975) Rank correlation methods, 4th edn. Charles Griffin, London
- Lettenmaier DP (1988) Multivariate nonparametric tests for trend in water quality. *Water Resour Bull* 24(3):505–512
- Li X, Ju H, Sarah G, Yan C, Batchelor WD, Liu Q (2017) Spatiotemporal variation of drought characteristics in the Huang-Huai-Hai Plain, China under the climate change scenario. *J Integr Agric* 16:2308–2322
- Li H, Liu L, Shan B, Xu Z, Niu Q, Cheng L, Liu X, Xu Z (2019) Spatiotemporal variation of drought and associated multi-scale response to climate change over the Yarlung Zangbo River Basin of Qinghai–Tibet Plateau, China. *Remote Sens* 11:1596
- Li BF, Chen YN, Shi X (2020) Does elevation dependent warming exist in high mountain Asia? *Environ Res Lett* 15:024012
- Ling HB, Xu HL, Guo B, Deng XY, Zhang P, Wang X (2019) Regulating water disturbance for mitigating drought stress to conserve and restore a desert riparian forest ecosystem. *J Hydrol* 572:659–670
- Ling HB, Guo B, Yan JJ, Deng XY, Xu HL, Zhang GP (2020) Enhancing the positive effects of ecological water conservancy engineering on desert riparian forest growth in an arid basin. *Ecol Indic* 118:106797
- Liu S, Zhang Y, Cheng F, Hou X, Zhao S (2017) Response of grassland degradation to drought at different time-scales in Qinghai Province: spatio-temporal characteristics, correlation, and implications. *Remote Sens* 9:1329
- Liu X, Pan Y, Zhu X, Yang T, Bai J, Sun Z (2018) Drought evolution and its impact on the crop yield in the North China Plain. *J Hydrol* 564: 984–996
- Mann HB (1945) Nonparametric tests against trend. *Econometrica* 13: 245–259
- Manzano A, Clemente MA, Morata A, Luna MY, Begueria S, Vicente-Serrano SM, Martin ML (2019) Analysis of the atmospheric circulation pattern effects over SPEI drought index in Spain. *Atmos Res* 230:11
- Marvel K, Cook BI, Bonfils CJ, Durack PJ, Smerdon JE, Williams AP (2019) Twentieth-century hydroclimate changes consistent with human influence. *Nature* 569:59
- McKee TB, Doesken NJ, Kleist J (1993) The relationship of drought frequency and duration to time scales. In: *Proceedings of the 8th Conference on Applied Climatology*, Anaheim, CA, USA, 17–23 January. vol 22. American Meteorological Society Boston, MA
- Mei XR et al (2013) Pathways to synchronously improving crop productivity and field water use efficiency in the North China Plain. *Sci Agric Sin* 46:1149–1157
- Palmer WC (1965) *Meteorological drought*, vol 58. US Weather Bureau, Washington
- Paulo A, Rosa R, Pereira L (2012) Climate trends and behaviour of drought indices based on precipitation and evapotranspiration in Portugal. *Nat Hazards Earth Syst Sci* 12:1481–1491
- Peña-Gallardo M, Vicente-Serrano S, Camarero J, Gazol A, Sánchez-Salguero R, Domínguez-Castro F, el Kenawy A, Beguería-Portugés S, Gutiérrez E, de Luis M, Sangüesa-Barreda G, Novak K, Rozas V, Tíscaer P, Linares J, Martínez del Castillo E, Ribas Matamoros M, García-González I, Silla F, Camisón Á, Génova M, Olano J, Longares L, Hevia A, Galván J (2018) Drought sensitivity on forest growth in peninsular Spain and the Balearic Islands. *Forests* 9:524
- Shiau JT, Feng S, Nadarajah S (2007) Assessment of hydrological droughts for the Yellow River, China, using copulas. *Hydrol Process* 21:2157–2163
- Su YZ, Guo B, Zhou ZT, Zhong YL, Min LL (2020) Spatio-temporal variations in groundwater revealed by GRACE and its driving factors in the Huang-Huai-Hai Plain, China. *Sensors* 20(3):922
- Tang GQ, Long D, Hong Y, Gao J, Wan W (2018) Documentation of multifactorial relationships between precipitation and topography of the Tibetan Plateau using spaceborne precipitation radars. *Remote Sens Environ* 208:82–96
- Um MJ, Kim Y, Park D, Jung K, Wang Z, Kim MM, Shin H (2020) Impacts of potential evapotranspiration on drought phenomena in different regions and climate zones. *Sci Total Environ* 703:13
- Van der Schrier G, Barichivich J, Briffa KR, Jones PD (2013) A scPDSI-based global data set of dry and wet spells for 1901–2009. *J Geophys Res-Atmos* 118:4025–4048
- Vicente-Serrano SM, Beguería S, López-Moreno JI (2010a) A multiscale drought index sensitive to global warming: the standardized precipitation evapotranspiration index. *J Clim* 23:1696–1718
- Vicente-Serrano SM, Beguería S, López-Moreno JI, Angulo M, El Kenawy A (2010b) A new global 0.5 gridded dataset (1901–2006) of a multiscale drought index: comparison with current drought index datasets based on the Palmer drought severity index. *J Hydrometeorol* 11:1033–1043
- Vicente-Serrano SM, Beguería S, Lorenzo-Lacruz J, Camarero JJ, López-Moreno JI, Azorin-Molina C, Revuelto J, Morán-Tejeda E, Sanchez-Lorenzo A (2012) Performance of drought indices for ecological, agricultural, and hydrological applications. *Earth Interact* 16:1–27
- Vicente-Serrano SM, Van der Schrier G, Beguería S, Azorin-Molina C, Lopez-Moreno J-I (2015) Contribution of precipitation and reference evapotranspiration to drought indices under different climates. *J Hydrol* 526:42–54
- Vicente-Serrano SM, Miralles DG, Domínguez-Castro F, Azorin-Molina C, el Kenawy A, McVicar TR, Tomás-Burguera M, Beguería S, Maneta M, Peña-Gallardo M (2018) Global assessment of the standardized evapotranspiration deficit index (SEDI) for drought analysis and monitoring. *J Clim* 31:5371–5393
- Vu MT, Raghavan SV, Pham DM, Liang S-Y (2015) Investigating drought over the Central Highland, Vietnam, using regional climate models. *J Hydrol* 526:265–273
- Wang Q, Shi P, Lei T, Geng G, Liu J, Mo X, Li X, Zhou H, Wu J (2015) The alleviating trend of drought in the Huang-Huai-Hai Plain of China based on the daily SPEI. *Int J Climatol* 35:3760–3769
- Wang F, Wang Z, Yang H, Zhao Y (2018) Study of the temporal and spatial patterns of drought in the Yellow River Basin based on SPEI. *Sci China-Earth Sci* 61:1098–1111
- Wang J, Yang Y, Huang J, Adhikari B (2019) Adaptive irrigation measures in response to extreme weather events: empirical evidence from the North China plain. *Reg Environ Chang* 19:1009–1022
- Wu D, Fang S, Li X, He D, Zhu Y, Yang Z, Xu J, Wu Y (2019) Spatial-temporal variation in irrigation water requirement for the winter wheat-summer maize rotation system since the 1980s on the North China Plain. *Agric Water Manag* 214:78–86
- Xiao L, Fang X, Zhang Y, Ye Y, Huang H (2014) Multi-stage evolution of social response to flood/drought in the North China Plain during 1644–1911. *Reg Environ Chang* 14:583–595
- Xiao L, Fang X, Zhao W (2018) Famine relief, public order, and revolts: interaction between government and refugees as a result of drought/flood during 1790–1911 in the North China Plain. *Reg Environ Chang* 18:1721–1730
- Xu CY, Gong L, Jiang T, Chen D, Singh V (2006) Analysis of spatial distribution and temporal trend of reference evapotranspiration and pan evaporation in Changjiang (Yangtze River) catchment. *J Hydrol* 327:81–93
- Xu FL, Guo B, Ye B, Ye Q, Chen H, Ju X, Guo J, Wang Z (2019) Systematical evaluation of GPM IMERG and TRMM 3B42V7 precipitation products in the Huang-Huai-Hai Plain, China. *Remote Sens* 11:697
- Yang J, Mei X, Huo Z, Yan C, Hui J, F-h Z, Qin L (2015) Water consumption in summer maize and winter wheat cropping system based on SEBAL model in Huang-Huai-Hai Plain, China. *J Integr Agric* 14:2065–2076
- Yang Y, Wang J, Huang J (2016) The adaptive irrigation behavior of farmers and impacts on yield during extreme drought events in the North China Plain. *Remote Sens* 38:900–908

- Yang H, Xiao H, Guo C, Sun Y (2019) Spatial-temporal analysis of precipitation variability in Qinghai Province, China. *Atmos Res* 228:242–260
- Yao JQ, Zhao Y, Chen YZ, Yu X, Zhang R (2018) Multi-scale assessments of droughts: a case study in Xinjiang, China. *Sci Total Environ* 630:444–452
- Ye Y, Fang X, Khan MAU (2012) Migration and reclamation in Northeast China in response to climatic disasters in North China over the past 300 years. *Reg Environ Chang* 12:193–206
- Ye L, Shi K, Zhang H, Xin Z, Hu J, Zhang C (2019) Spatio-temporal analysis of drought indicated by SPEI over Northeastern China. *Water* 11:908
- Yuan Y, Yan D, Yuan Z, Yin J, Zhao Z (2019) Spatial distribution of precipitation in Huang-Huai-Hai River Basin between 1961 to 2016, China. *Int J Environ Res Public Health* 16:3404
- Zhang Y, You Q, Chen C, Ge J, Adnan M (2017) Evaluation of down-scaled CMIP5 coupled with VIC model for flash drought simulation in a humid subtropical basin, China. *J Clim* 31:1075–1090
- Zhang Y, Li G, Ge J, Li Y, Yu Z, Niu H (2019a) sc_PDSI is more sensitive to precipitation than to reference evapotranspiration in China during the time period 1951–2015. *Ecol Indic* 96:448–457
- Zhang Y, Liu C, You Q, Chen C, Xie W, Ye Z, Li X, He Q (2019b) Decrease in light precipitation events in Huai River Eco-economic Corridor, a climate transitional zone in eastern China. *Atmos Res* 226:240–254
- Zhang Y, Mao G, Chen C, Lu Z, Luo Z, Zhou W (2020) Population exposure to concurrent daytime and nighttime heatwaves in Huai River Basin, China. *Sust Cities Soc*:102309
- Zhao Y, Xu X, Huang W, Wang Y, Xu Y, Chen H, Kang Z (2019) Trends in observed mean and extreme precipitation within the Yellow River Basin, China. *Theor Appl Climatol* 136:1387–1396
- Zhou ZT, Guo B, Su YZ, Chen ZS, Wang J (2020) Multidimensional evaluation of TRMM 3B43V7 satellite-based precipitation product in mainland China from 1998–2016. *Peer J* 8:e8615
- Zhu Y, Chang J, Huang S, Huang Q (2015) Characteristics of integrated droughts based on a nonparametric standardized drought index in the Yellow River Basin, China. *Hydrol Res* 47:454–467

Publisher's note Springer Nature remains neutral with regard to jurisdictional claims in published maps and institutional affiliations.